

Research Article

Cosmological Evolution of Pilgrim Dark Energy in $f(G)$ Gravity

Abdul Jawad and Shamaila Rani

Department of Mathematics, COMSATS Institute of Information Technology, Lahore 54000, Pakistan

Correspondence should be addressed to Abdul Jawad; jawadab181@yahoo.com

Received 4 January 2015; Revised 21 February 2015; Accepted 1 March 2015

Academic Editor: Elias C. Vagenas

Copyright © 2015 A. Jawad and S. Rani. This is an open access article distributed under the Creative Commons Attribution License, which permits unrestricted use, distribution, and reproduction in any medium, provided the original work is properly cited. The publication of this article was funded by SCOAP³.

We analyze the behavior of pilgrim dark energy with Hubble horizon in $f(G)$ gravity. We reconstruct the $f(G)$ models through correspondence phenomenon by assuming two values of pilgrim dark energy parameter ($u = 2, -2$). We evaluate the equation of state parameter which shows evolution of the universe in the quintessence, vacuum, and phantom phase for both cases of u and give favor the pilgrim dark energy phenomenon. Also, squared speed of sound exhibits the stability of $f(G)$ model for both cases of u . The $w_{\text{PDE}} - w'_{\text{PDE}}$ also provides freezing and thawing regions in this scenario. In this framework, the r - s plane also corresponds to different dark energy scenarios.

1. Introduction

It is confirmed through different observational schemes that our universe undergoes accelerated expansion. The pioneer observations about this accelerated expansion phenomenon was made by a variety of astronomers through supernova type Ia [1, 2]. The subsequent attempts in this regard also favor this phenomenon [3–6]. The background force which acts upon behind this phenomenon is an exotic type called dark energy (DE) whose nature is still under consideration. In order to understand its nature, various approaches have been adopted, the proposal of different dynamical DE models [7–14] and modified theories of gravity [15–19] to peruse the DE problem.

Moreover, the accelerated expansion is also discussed widely in the literature through correspondence phenomenon of dynamical DE models with modified gravity. Many works have been done in this direction by adopting different scenarios in modified gravity theories [20–25]. Further, Setare and Saridakis [26] considered the holographic and Gauss-Bonnet DE models separately to investigate the conditions under which these models can be simultaneously valid. They found that this correspondence phenomenon leads to accelerated expansion of the universe. Also, they investigated the correspondence of HDE model with canonical, phantom, and quintom models minimally coupled to gravity

and pointed out consistent results about acceleration of the universe [27]. Further, Setare [28–32] has studied this correspondence scenario incorporating different dynamical DE models as well as modified theories of gravity in this respect. We have also investigated the correspondence phenomenon of various DE models with modified gravities and found that these scenarios favor the accelerated expansion phenomenon of the universe [33–39].

The bound of energy density as suggested by Cohen et al. [40] predicts the formation of black hole (BH) in quantum gravity. However, it is suggested that formation of BH can be avoided through appropriate repulsive force which resists the matter collapse phenomenon. This force can only provide phantom DE in spite of other phases of DE like vacuum and quintessence DE. By keeping in mind this phenomenon, Wei [41] has suggested the DE model called pilgrim DE (PDE) on the speculation in which phantom DE possesses the large negative pressure as compared to the quintessence DE which helps in violating the null energy condition and possibly prevent the formation of BH. In the past, many applications of phantom DE exist in the literature. For instance, phantom DE also plays an important role on the reduction of masses of BHs [42–45] and in the wormhole physics where the event horizon can be avoided due to its presence [46–50].

In the present work, we present the reconstruction scenario of newly proposed DE model called pilgrim DE (PDE)

with the $f(G)$ gravity. We will construct $f(G)$ models and analyze it through different cosmological parameters as well as cosmological planes. The paper is organized as follows: next section contains the discussion of $f(G)$ models. In Section 3, we provide the analysis of EoS parameter, squared speed of sound, $w_{\text{PDE}}-w'_{\text{PDE}}$, and r - s planes. The last section contains the summary of the outcomes.

2. Pilgrim Dark Energy $f(G)$ Models

It was demonstrated by Sahni and Starobinsky [51] that there is also a possibility to write the field equations in modified gravities in terms of usual Einstein field equations by transferring all additional terms from the left-hand side into the right-hand side of the Einstein equations and called them as an effective energy momentum tensor of DE. Here, we consider $f(G)$ gravity where the modified field equations are [51, 52]

$$3H^2 = \rho_G + \rho_m, \quad 2\dot{H} + 3H^2 = p_G + p_m. \quad (1)$$

The subscripts m indicate the matter contribution of energy density and pressure and $H = \dot{a}/a$ is the Hubble parameter with dot representing the time derivative. The Gauss-Bonnet invariant G for FRW metric becomes $G = 24H^2(\dot{H} + H^2)$. Also,

$$\begin{aligned} \rho_G &= \rho_m + Gf_G - f - 24H^3 \dot{f}_G, \\ p_G &= -8H^2 \ddot{f}_G - 16H(H^2 + \dot{H}) \dot{f}_G - f + Gf_G. \end{aligned} \quad (2)$$

Here, we will incorporate with the pressureless matter, that is, $p_m = 0$, while the energy density of matter ρ_m satisfies the following energy conservation equation:

$$\dot{\rho}_m + 3H\rho_m = 0. \quad (3)$$

This equation has a solution which is given by the following expression:

$$\rho_m = \rho_{m0} a^{-3}, \quad (4)$$

where ρ_{m0} is an arbitrary constant.

It is predicted that phantom DE with strong negative pressure can push the universe towards the big rip singularity where all the physical objects lose the gravitational bounds and finally dispersed. This prediction supports the phenomenon of the avoidance of BH formation and motivated Wei [41] in constructing PDE model. The PDE model is defined as

$$\rho_{\text{PDE}} = 3n^2 m_p^{4-s} L^{-u}, \quad (5)$$

where L is the IR cutoff and size of the system, u is the PDE parameter, n is conventional constant, and m_p is reduced Planck mass. Wei analyzed the PDE model through different possible theoretical and observational ways to make the BH-free phantom universe with Hubble horizon ($L = H^{-1}$) through PDE parameter (u). Further, Sharif and Jawad [43–45] have analyzed this proposal in detail by choosing different

IR cutoffs through well-known cosmological parameters in flat and nonflat universes. This model has also been in different modified gravities [53, 54].

Here, we make correspondence between PDE and $f(G)$ model by equating their energy densities; that is, $\rho_G = \rho_{\text{PDE}}$. It yields

$$\begin{aligned} f - 24H^2(H^2 + \dot{H})f_G + (24)^2 H^4 \\ \cdot (2\dot{H}^2 + H\ddot{H} + 4H^2\dot{H})f_{GG} = -3n^2 m_p^{4-s} H^u. \end{aligned} \quad (6)$$

To find out an analytic solution of (6), we assume a power-law form of the scale factor as follows:

$$a(t) = a_0 t^m, \quad (7)$$

where the constant a_0 represents the present day value of the scale factor. By using (7) in the reconstructed equation, we obtain

$$\begin{aligned} G^2 \frac{d^2 f(G)}{dG^2} + \frac{(m-1)^2}{4} G \frac{df(G)}{dG} - \frac{(m-1)^2}{4} f(G) \\ = \frac{n^2}{32m^{2u}(m-1)^{(u-8)/4}} G^u. \end{aligned} \quad (8)$$

Equation (8) is a second-order linear differential equation whose solution is given by

$$f(G) = \frac{G^u (m-1)^{0.25(8-u)} m^{-2u} n^2}{32(l^+ - 2u)(l^- - 2u)} + AG^{l^-} + BG^{l^+}, \quad (9)$$

where A and B are integration constants and

$$l^\pm = \frac{1}{2} \left(1 \pm \sqrt{1 + \frac{1}{2}(m-1)^2 + \frac{1}{16}(m-1)^4} - \frac{1}{4}(m-1)^2 \right). \quad (10)$$

Equation (9) represents the reconstructed PDE $f(G)$ model which we have plotted for three different values of $m = 2, 2.2,$ and 2.4 as shown in Figures 1 and 2. The assumptions of other constants parameters are $A = 0.5, B = 0.2, n = 0.91$. Figure 1 shows that the $f(G)$ model versus G exhibits decreasing behavior initially and then approaches $G = 0$ after some interval. After that, it shows increasing behavior forever for all values of m . Figure 2 represents that the reconstructed function $f(G)$ shows rapid decrease initially and then approaches positive value forever for all values of m .

3. Cosmological Analysis of PDE $f(G)$ Models

In this section, we discuss the cosmological parameters such as EoS parameter and squared speed of sound. Also, we develop cosmological planes such as $w_{\text{PDE}}-w'_{\text{PDE}}$ and r - s .

3.1. Equation of State Parameter. Through reconstruction scenario, that is, $\rho_G = \rho_{\text{PDE}}$ and $p_G = p_{\text{PDE}}$, we can get EoS as follows:

$$w_{\text{PDE}} = \frac{p_{\text{PDE}}}{\rho_{\text{PDE}}}. \quad (11)$$

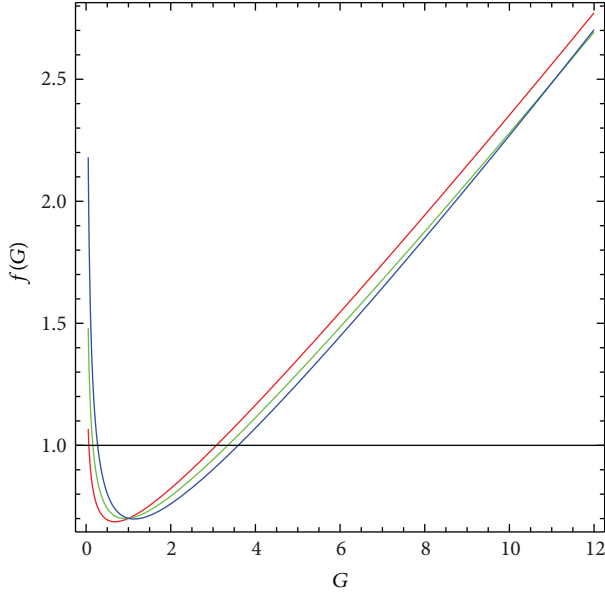


FIGURE 1: Plot of $f(G)$ versus G for PDE parameter $u = 2$ with $m = 2$ (red), $m = 2.2$ (green), and $m = 2.4$ (blue).

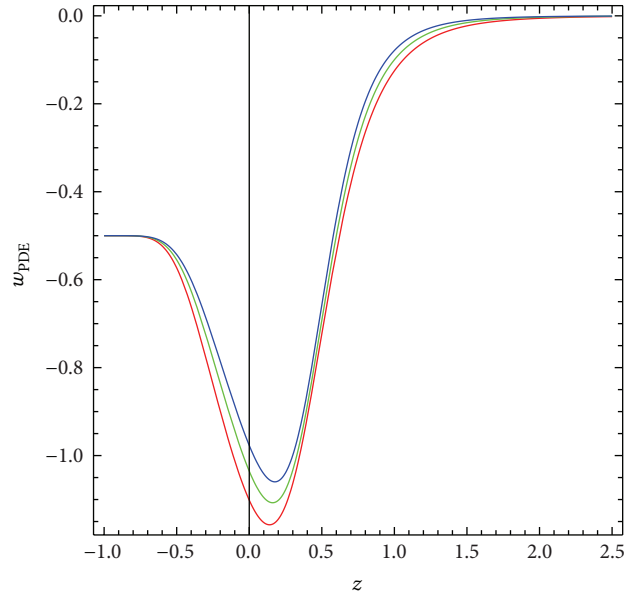


FIGURE 3: Plot of w_{PDE} versus z for PDE parameter $u = 2$ with $m = 2$ (red), $m = 2.2$ (green), and $m = 2.4$ (blue).

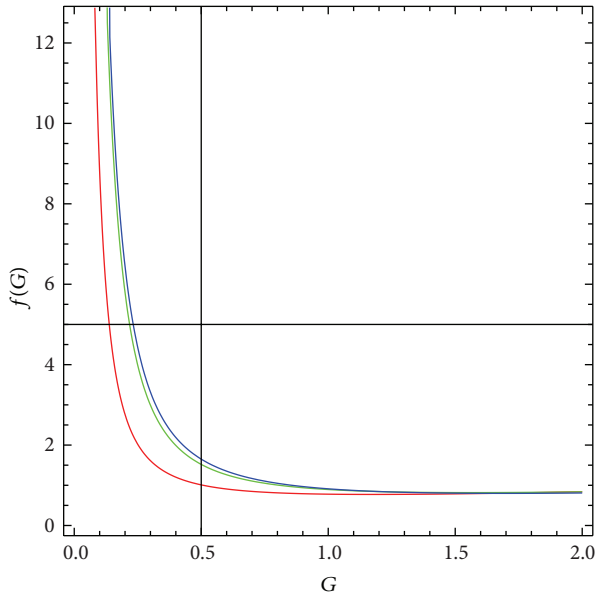


FIGURE 2: Plot of $f(G)$ versus G for PDE parameter $u = -2$ with $m = 2$ (red), $m = 2.2$ (green), and $m = 2.4$ (blue).

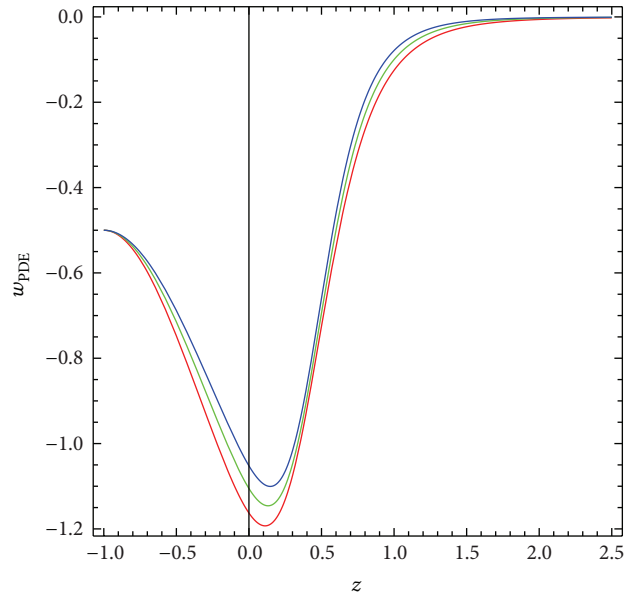


FIGURE 4: Plot of w_{PDE} versus z for PDE parameter $u = -2$ with $m = 2$ (red), $m = 2.2$ (green), and $m = 2.4$ (blue).

We plot the above EoS parameter versus redshift parameter z for PDE parameter $u = 2, -2$ as shown in Figures 3 and 4, respectively, while keeping the other constants same as in previous section. We use the expression of scale factor in terms of redshift parameter $a = a_0(1+z)^{-1}$. It can be observed from Figure 3 ($u = 2$) that the EoS parameter starts from quintessence phase (at the present time), crosses the phantom divide line, and then goes towards phantom phase of the universe. After achieving the extreme value of phantom phase, the EoS parameter turns back and approaches dust like

matter in the end. This type of behavior of EoS parameter is termed as quintom. Figure 4 ($u = -2$) shows similar behavior of EoS parameter as in case of $u = 2$. It is concluded that both PDE $f(G)$ models favor the PDE phenomenon.

3.2. Squared Speed of Sound. Here, we analyze the squared speed of sound for the stability analysis of PDE $f(G)$ model. In the present case, the squared speed of sound takes the form

$$v_s^2 = \frac{\dot{P}_{\text{PDE}}}{\dot{\rho}_{\text{PDE}}}. \quad (12)$$

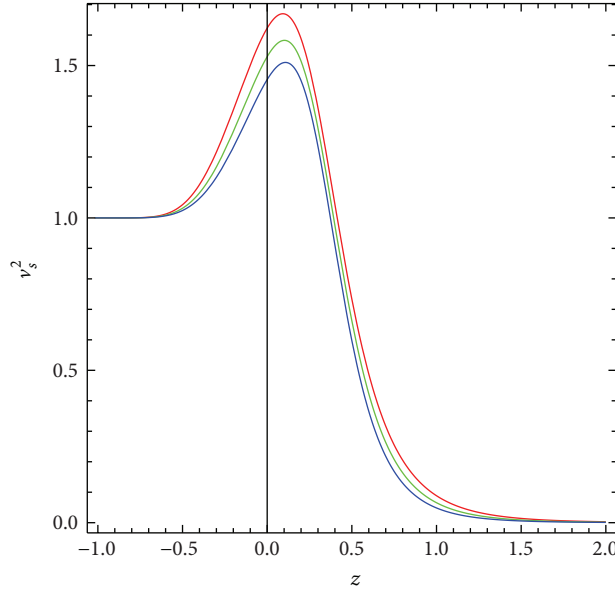


FIGURE 5: Plot of v_s^2 versus z for PDE parameter $u = 2$ with $m = 2$ (red), $m = 2.2$ (green), and $m = 2.4$ (blue).

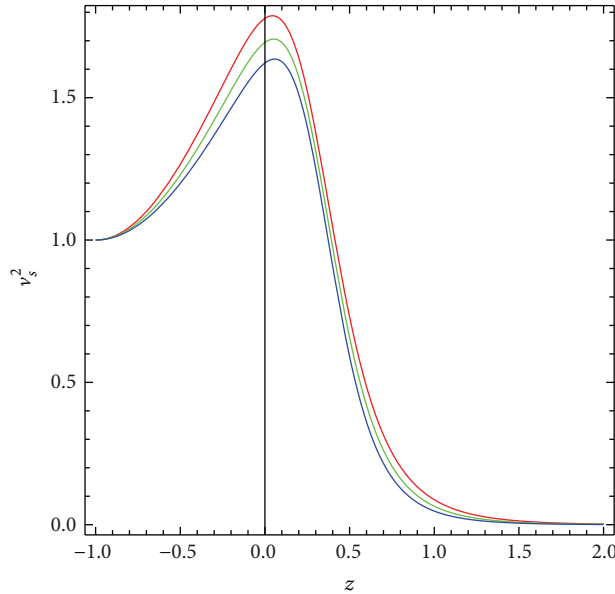


FIGURE 6: Plot of v_s^2 versus z for PDE parameter $u = -2$ with $m = 2$ (red), $m = 2.2$ (green), and $m = 2.4$ (blue).

The sign of v_s^2 is very important to see the stability of background evolution of the model. A positive value indicates a stable model whereas instability of a given perturbation corresponds to the negative value of v_s^2 . The plot of squared speed of sound with respect to redshift parameter for two values of PDE parameter is as shown in Figures 5 and 6. It can be observed from Figures 5 and 6 that the PDE $f(G)$ model for $u = 2, -2$ shows stability at the present as well as at latter epoch because $v_s^2 \geq 0$ for all the time.

3.3. w_{PDE} - w'_{PDE} Plane. This plane is firstly proposed by Caldwell and Linder [55] and tested the behavior of quintessence scalar field DE model through this plane. Also, this can be

divided into two regions such as thawing and freezing. The thawing region is described as ($\omega'_\Lambda > 0, \omega_\Lambda < 0$) while freezing region as ($\omega'_\Lambda < 0, \omega_\Lambda < 0$). Here, we develop the w_{PDE} - w'_{PDE} plane for reconstructed PDE $f(G)$ models corresponding to $u = 2, -2$ as shown in Figures 7 and 8, respectively, for three different values of $m = 2, 2.2$, and 2.4 . It can be observed from Figure 7 that w_{PDE} - w'_{PDE} plane corresponds to freezing region only for $m = 2, 2.4$ while it lies in both regions (freezing and thawing) for $m = 2.2$. However, w_{PDE} - w'_{PDE} plane corresponds to thawing region only for all cases of m . Hence, w_{PDE} - w'_{PDE} planes corresponding to $m = 2, 2.2, 2.4$ show consistency with the accelerated expansion of the universe.

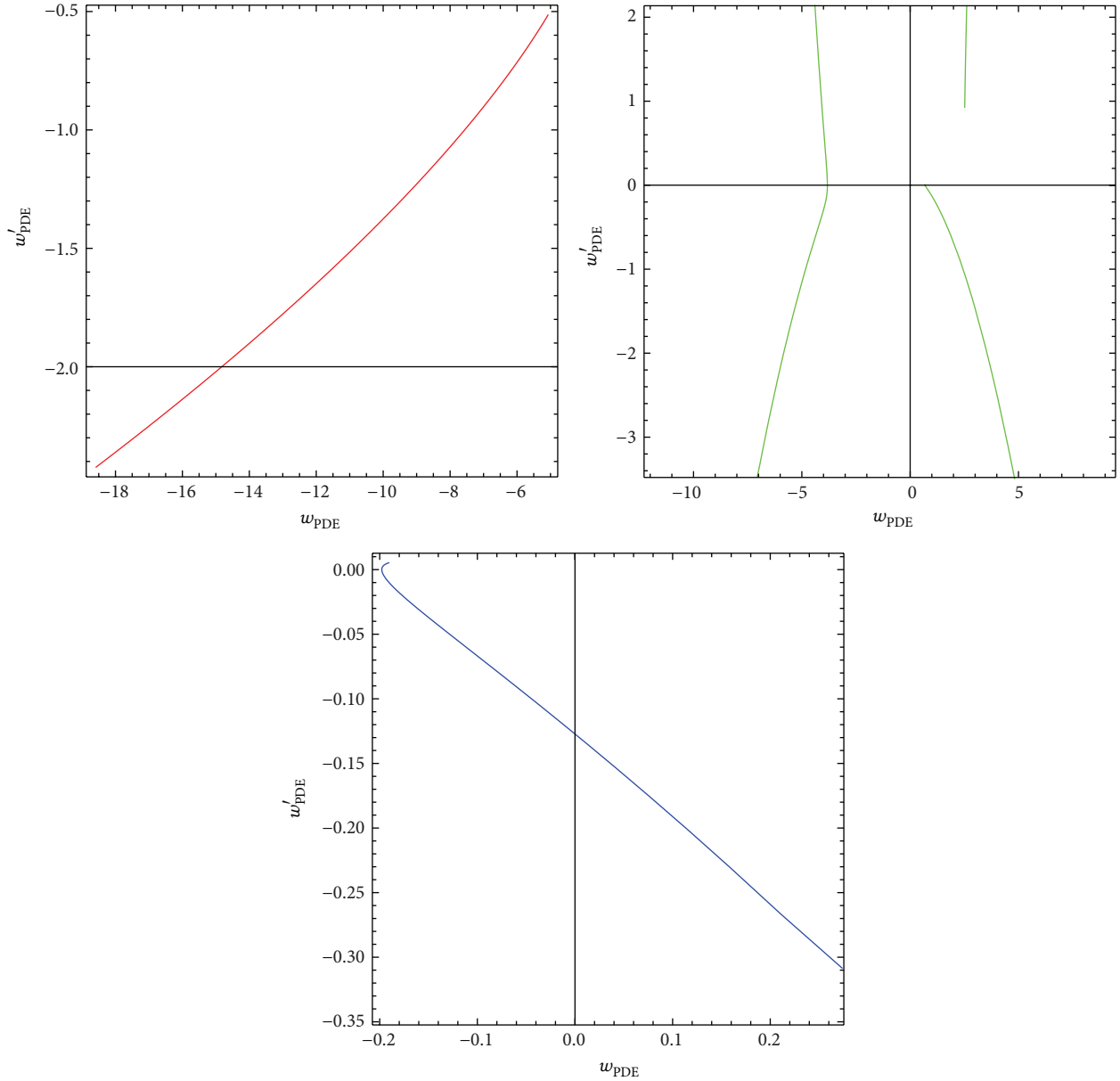


FIGURE 7: Trajectories of $w_{\text{PDE}} - w'_{\text{PDE}}$ for reconstructed PDE $f(G)$ model for $u = 2$ with $m = 2$ (red), $m = 2.2$ (green), and $m = 2.4$ (blue).

3.4. r - s Plane. Up to now, a variety of DE models have been developed for explaining the phenomenon of DE in the accelerated expansion of the universe. It is necessary to differentiate these models so that one can decide which one provides better explanation for the current status of the universe. Many DE models give the same present value of the deceleration and Hubble parameter, so these parameters could not be able to discriminate the DE models. For this purpose, Sahni et al. [56] introduced two new dimensionless parameters by combining the Hubble and deceleration parameters which are expressed as

$$r = \frac{\ddot{a}}{aH^3}, \quad s = \frac{r-1}{3(q-1/2)}, \quad (13)$$

where

$$q = -\frac{\ddot{a}}{aH^2} = -\left(1 + \frac{\dot{H}}{H^2}\right). \quad (14)$$

The statefinders are useful in the sense that we can find the distance of a given DE model from Λ CDM limit. The well-known regions described by these cosmological parameters are as follows: $(r, s) = (1, 0)$ indicates Λ CDM limit and $(r, s) = (1, 1)$ shows CDM limit, while $s > 0$ and $r < 1$ represent the region of phantom and quintessence DE eras.

The r - s planes develop corresponding to reconstructed PDE $f(G)$ models with $u = 2, -2$ for three different values of $m = 2, 2.2,$ and 2.4 as shown in Figures 9 and 10. Figure 9 shows that r - s plane (PDE $f(G)$ models with

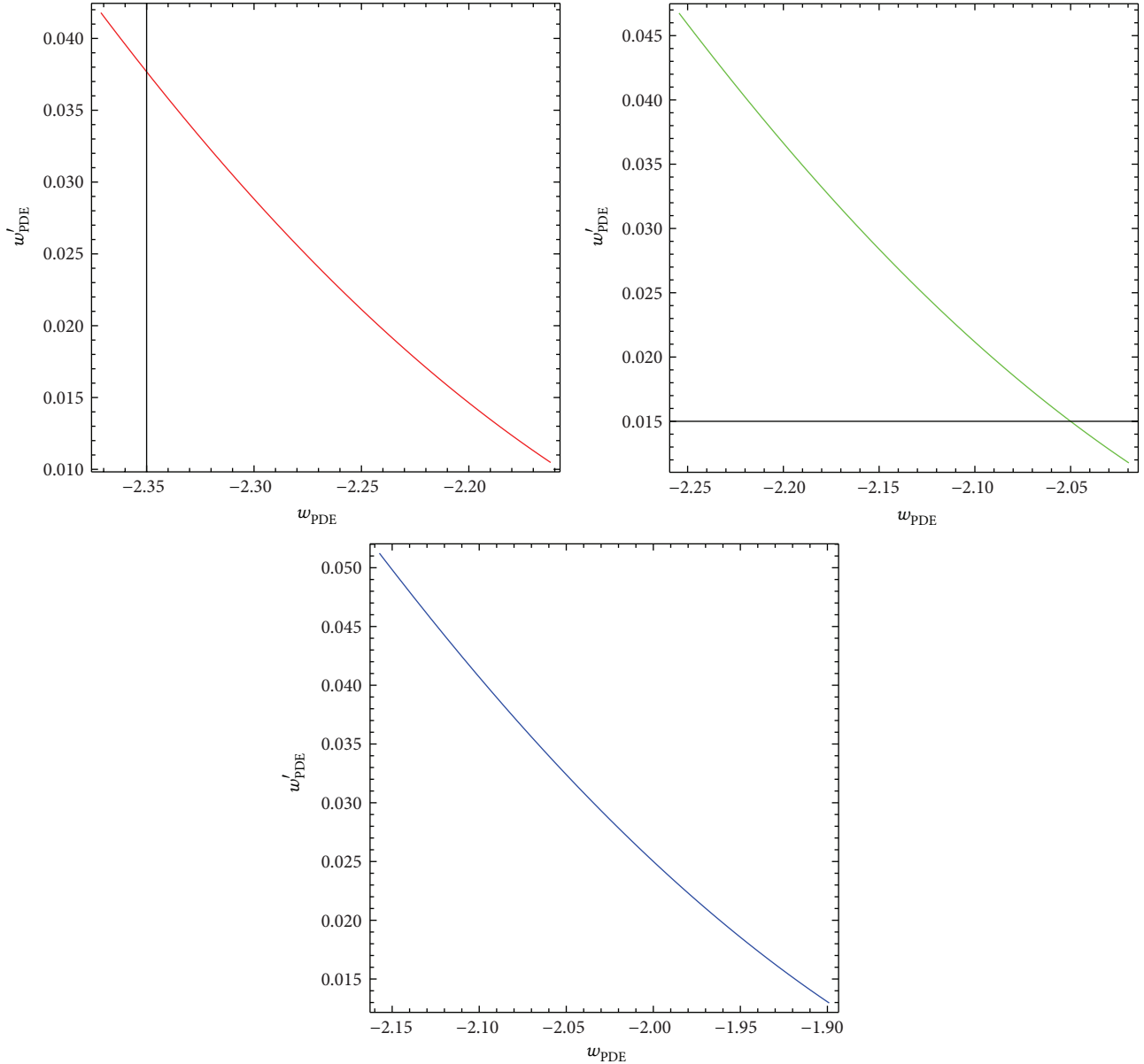


FIGURE 8: Trajectories of $w_{\text{PDE}}-w'_{\text{PDE}}$ for reconstructed PDE $f(G)$ model for $u = -2$ with $m = 2$ (red), $m = 2.2$ (green), and $m = 2.4$ (blue).

$u = 2$) corresponds to Chaplygin gas model and DE regions (quintessence and phantom) for all three cases of m . Also, r - s plane (PDE $f(G)$ models with $u = -2$) corresponds to only Chaplygin gas model as shown in Figure 10 in all three cases of m . However, Λ CDM limit can not be achieved in both cases of PDE parameter of u .

4. Concluding Remarks

In this paper, we have considered the reconstruction phenomenon of a well-known PDE model with $f(G)$ gravity in the presence of power law scale factor. We have reconstructed $f(G)$ models with respect to two values of PDE parameter; that is, $u = 2, -2$. To check the significant cosmological aspects of these reconstructed models, we have presented

the analysis of different cosmological parameters as well as cosmological planes. We summarized the results of them as follows.

- (i) The $f(G)$ model versus G exhibits decreasing behavior initially and then approaches $G = 0$ after some interval as shown in Figure 1. After that, it shows increasing behavior forever for all values of m . Figure 2 represents that the reconstructed function $f(G)$ shows rapid decrease initially and then approaches positive value forever for all values of m .
- (ii) It can be observed from Figure 3 ($u = 2$) that the EoS parameter starts from quintessence phase (at the present time), crosses the phantom divide line, and then goes towards phantom phase of the universe.

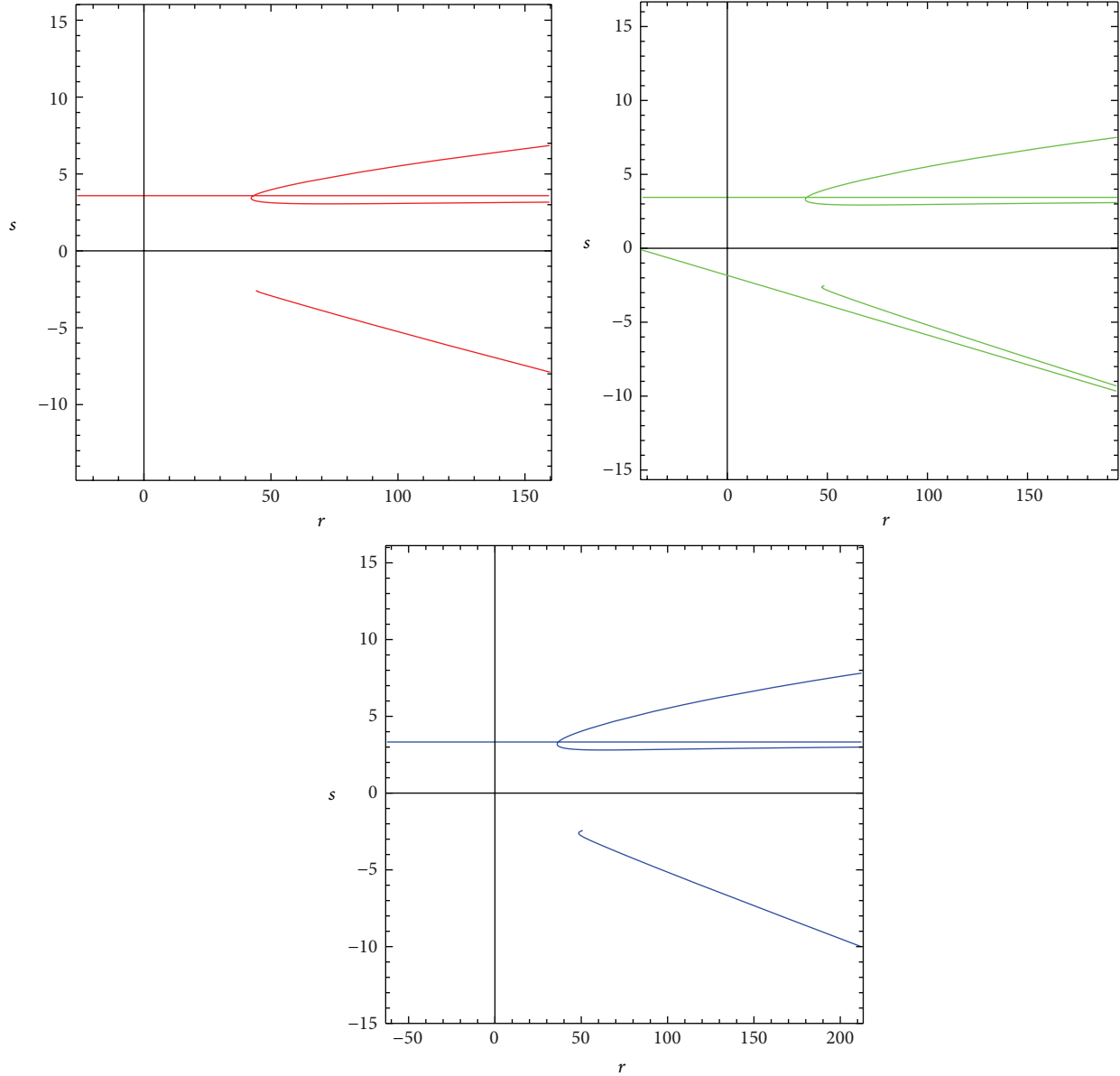


FIGURE 9: Trajectories of r - s for reconstructed PDE $f(G)$ model for $u = 2$ with $m = 2$ (red), $m = 2.2$ (green), and $m = 2.4$ (blue).

After achieving the extreme value of phantom phase, the EoS parameter turns back and approaches dust-like matter in the end. This type of behavior of EoS parameter is termed as quintom. Figure 4 ($u = -2$) shows similar behavior of EoS parameter as in case of $u = 2$. It is concluded that both PDE $f(G)$ models favor the PDE phenomenon.

- (iii) The plot of squared speed of sound with respect to redshift parameter for two values of PDE parameter is as shown in Figures 5 and 6. It can be observed from Figures 5 and 6 that the PDE $f(G)$ model for $u = 2, -2$ shows stability at the present as well as at latter epoch because $v_s^2 \geq 0$ for all the time.
- (iv) It can be observed from Figure 7 that $\omega_{\text{PDE}} - \omega'_{\text{PDE}}$ plane corresponds to freezing region only for $m = 2, 2.4$

while it lies in both regions (freezing and thawing) for $m = 2.2$. However, $\omega_{\text{PDE}} - \omega'_{\text{PDE}}$ plane corresponds to thawing region only for all cases of m . Hence, $\omega_{\text{PDE}} - \omega'_{\text{PDE}}$ planes corresponding to $m = 2, 2.2$, and 2.4 show consistency with the accelerated expansion of the universe.

- (v) Figure 9 shows that r - s plane (PDE $f(G)$ models with $u = 2$) corresponds to Chaplygin gas model and DE regions (quintessence and phantom) for all three cases of m . Also, r - s plane (PDE $f(G)$ models with $u = -2$) corresponds to only Chaplygin gas model as shown in Figure 10 in all three cases of m . However, Λ CDM limit can not be achieved in both cases of PDE parameter of u .

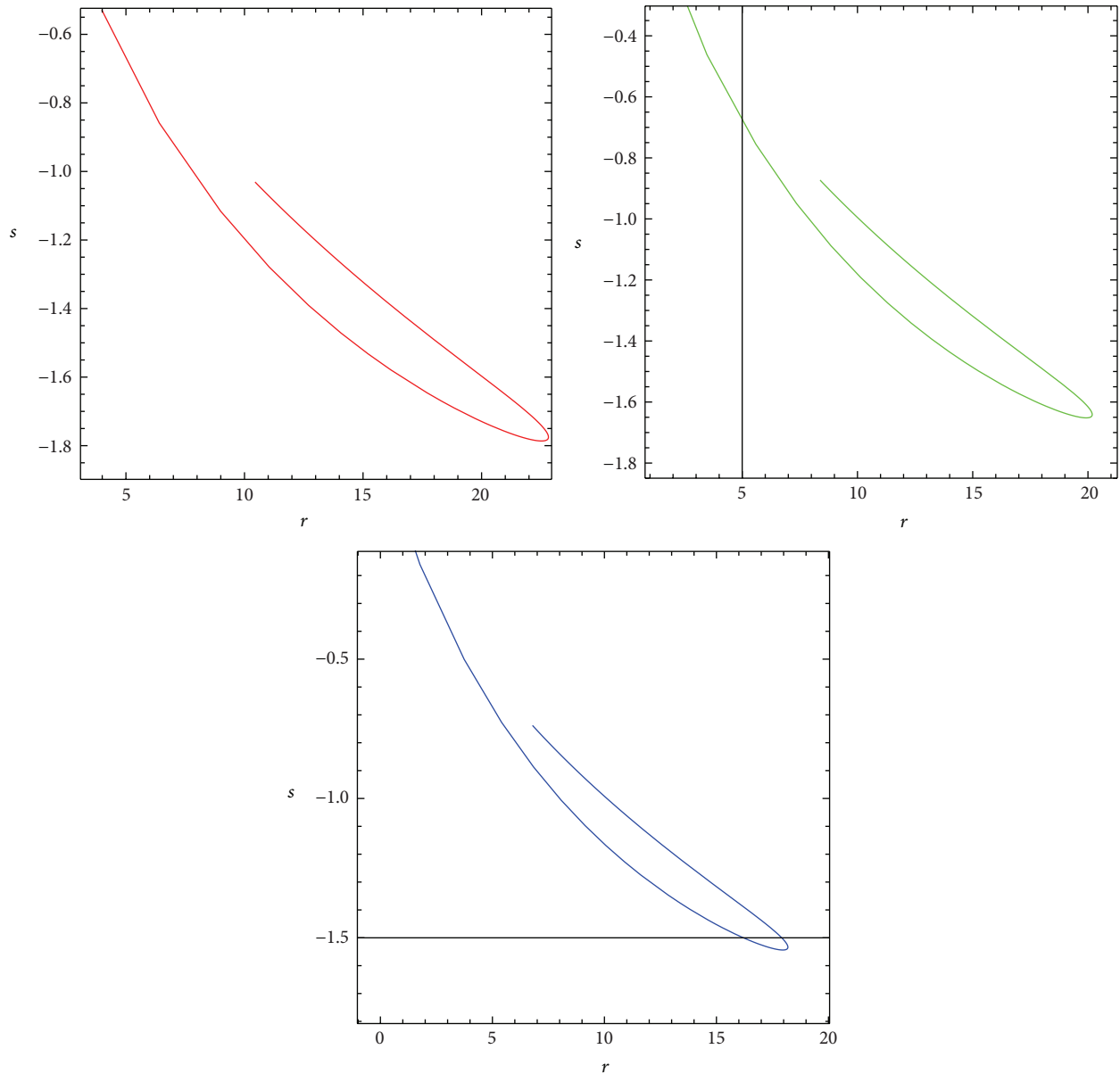


FIGURE 10: Trajectories of r - s for reconstructed PDE $f(G)$ model for $u = -2$ with $m = 2$ (red), $m = 2.2$ (green), and $m = 2.4$ (blue).

Conflict of Interests

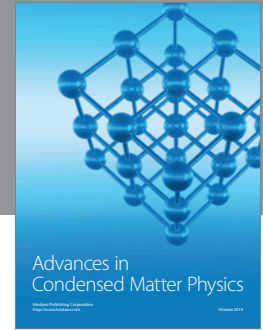
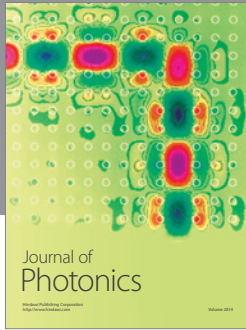
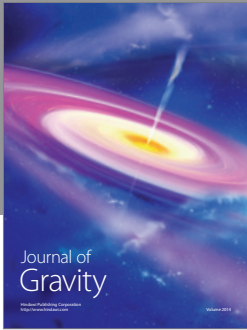
The authors declare that there is no conflict of interests regarding the publication of this paper.

References

- [1] A. G. Riess, A. V. Filippenko, P. Challis et al., "Observational evidence from supernovae for an accelerating universe and a cosmological constant," *The Astronomical Journal*, vol. 116, p. 1009, 1998.
- [2] S. Perlmutter, G. Aldering, G. Goldhaber et al., "Measurements of omega and lambda from 42 high-redshift supernovae," *The Astrophysical Journal*, vol. 517, no. 2, p. 565, 1999.
- [3] R. R. Caldwell and M. Doran, "Cosmic microwave background and supernova constraints on quintessence: concordance regions and target models," *Physical Review D*, vol. 69, Article ID 103517, 2004.
- [4] T. Koivisto and D. F. Mota, "Dark energy anisotropic stress and large scale structure formation," *Physical Review D*, vol. 73, no. 8, Article ID 083502, 12 pages, 2006.
- [5] S. F. Daniel, R. R. Caldwell, A. Cooray, and A. Melchiorri, "Large scale structure as a probe of gravitational slip," *Physical Review D*, vol. 77, no. 10, Article ID 103513, 12 pages, 2008.
- [6] H. Hoekstra and B. Jain, "Weak gravitational lensing and its cosmological applications," *Annual Review of Nuclear and Particle Science*, vol. 58, pp. 99–123, 2008.
- [7] C. Armendariz-Picon, T. Damour, and V. Mukhanov, " k -Inflation," *Physics Letters B*, vol. 458, no. 2-3, pp. 209–218, 1999.

- [8] R. R. Caldwell, "A phantom menace? Cosmological consequences of a dark energy component with super-negative equation of state," *Physics Letters B*, vol. 545, no. 1-2, pp. 23–29, 2002.
- [9] J. S. Bagla, H. K. Jassal, and T. Padmanabhan, "Cosmology with tachyon field as dark energy," *Physical Review D*, vol. 67, no. 6, Article ID 063504, 2003.
- [10] S. D. H. Hsu, "Entropy bounds and dark energy," *Physics Letters B*, vol. 594, no. 1-2, pp. 13–16, 2004.
- [11] M. Li, "A model of holographic dark energy," *Physics Letters B*, vol. 603, no. 1-2, pp. 1–5, 2004.
- [12] B. Feng, X. L. Wang, and X. M. Zhang, "Dark energy constraints from the cosmic age and supernova," *Physics Letters B*, vol. 607, pp. 35–41, 2005.
- [13] X. Zhang, F. Q. Wu, and J. Zhang, "New generalized Chaplygin gas as a scheme for unification of dark energy and dark matter," *Journal of Cosmology and Astroparticle Physics*, vol. 2006, no. 1, article 003, 2006.
- [14] R.-G. Cai, "A dark energy model characterized by the age of the universe," *Physics Letters B*, vol. 657, no. 4-5, pp. 228–231, 2007.
- [15] C. H. Brans and R. H. Dicke, "Mach's principle and a relativistic theory of gravitation," *Physical Review Letters*, vol. 124, p. 925, 1961.
- [16] E. V. Linder, "Einstein's other gravity and the acceleration of the Universe," *Physical Review D*, vol. 81, Article ID 127301, 2010.
- [17] S. Dutta and E. N. Saridakis, "Observational constraints on Hořava-Lifshitz cosmology," *Journal of Cosmology and Astroparticle Physics*, vol. 2010, no. 1, article 13, 2010.
- [18] M. Sharif and S. Rani, "Generalized teleparallel gravity via some scalar field dark energy models," *Astrophysics and Space Science*, vol. 345, no. 1, pp. 217–223, 2013.
- [19] M. Sharif and S. Rani, "Nonlinear electrodynamics in $f(T)$ gravity and generalized second law of thermodynamics," *Astrophysics and Space Science*, vol. 346, no. 2, pp. 573–582, 2013.
- [20] S. Nojiri and S. D. Odintsov, "Modified Gauss-Bonnet theory as gravitational alternative for dark energy," *Physics Letters B*, vol. 631, no. 1-2, pp. 1–6, 2005.
- [21] S. Nojiri and S. D. Odintsov, "Modified $f(R)$ gravity consistent with realistic cosmology: from a matter dominated epoch to a dark energy universe," *Physical Review D*, vol. 74, Article ID 086005, 2006.
- [22] S. Nojiri, S. D. Odintsov, and H. Štefančić, "Transition from a matter-dominated era to a dark energy universe," *Physical Review D*, vol. 74, no. 8, Article ID 086009, 9 pages, 2006.
- [23] S. Nojiri and S. D. Odintsov, "Modified gravity and its reconstruction from the universe expansion history," *Journal of Physics: Conference Series*, vol. 66, Article ID 012005, 2007.
- [24] S. Nojiri, S. D. Odintsov, and D. Diego Sez-Gmez, "Cosmological reconstruction of realistic modified $F(R)$ gravities," *Physics Letters B*, vol. 681, pp. 74–80, 2009.
- [25] S. Nojiri and S. D. Odintsov, "Unified cosmic history in modified gravity: from $F(R)$ theory to Lorentz non-invariant models," *Physics Reports*, vol. 505, no. 2–4, pp. 59–144, 2011.
- [26] M. R. Setare and E. N. Saridakis, "Correspondence between holographic and Gauss-Bonnet dark energy models," *Physics Letters B*, vol. 670, no. 1, pp. 1–4, 2008.
- [27] M. R. Setare and E. N. Saridakis, "Coupled oscillators as models of quintom dark energy," *Physics Letters, Section B: Nuclear, Elementary Particle and High-Energy Physics*, vol. 668, no. 3, pp. 177–181, 2008.
- [28] M. R. Setare, "Bulk-brane interaction and holographic dark energy," *Physics Letters B*, vol. 642, no. 5-6, pp. 421–425, 2006.
- [29] M. R. Setare, "The holographic dark energy in non-flat Brans-Dicke cosmology," *Physics Letters B*, vol. 644, no. 2-3, pp. 99–103, 2007.
- [30] M. R. Setare, "Interacting holographic phantom," *The European Physical Journal C*, vol. 50, no. 4, pp. 991–998, 2007.
- [31] M. R. Setare, "Holographic modified gravity," *International Journal of Modern Physics D*, vol. 17, no. 12, pp. 2219–2228, 2008.
- [32] M. R. Setare, D. Momeni, and S. K. Moayedi, "Interacting dark energy in Hořava-Lifshitz cosmology," *Astrophysics and Space Science*, vol. 338, no. 2, pp. 405–410, 2012.
- [33] A. Jawad, A. Pasqua, and S. Chattopadhyay, "Correspondence between $f(G)$ gravity and holographic dark energy via power-law solution," *Astrophysics and Space Science*, vol. 344, no. 2, pp. 489–494, 2013.
- [34] A. Jawad, S. Chattopadhyay, and A. Pasqua, "Reconstruction of $f(G)$ gravity with the new agegraphic dark-energy model," *The European Physical Journal Plus*, vol. 128, article 88, 2013.
- [35] A. Jawad, A. Pasqua, and S. Chattopadhyay, "Holographic reconstruction of $f(G)$ gravity for scale factors pertaining to emergent, logamediate and intermediate scenarios," *The European Physical Journal Plus*, vol. 128, p. 156, 2013.
- [36] A. Jawad, S. Chattopadhyay, and A. Pasqua, "A holographic reconstruction of the modified $f(R)$ Horava-Lifshitz gravity with scale factor in power-law form," *Astrophysics and Space Science*, vol. 346, no. 1, pp. 273–278, 2013.
- [37] A. Jawad, S. Chattopadhyay, and A. Pasqua, "Power-law solution of new agegraphic modified $f(R)$ Horava-Lifshitz gravity," *The European Physical Journal Plus*, vol. 129, article 51, 2014.
- [38] A. Jawad, "Reconstruction of TeX models via well-known scale factors," *The European Physical Journal Plus*, vol. 129, article 207, 2014.
- [39] A. Jawad, "Analysis of QCD ghost $F(\tilde{R})$ gravity," *Astrophysics and Space Science*, vol. 353, pp. 691–698, 2014.
- [40] A. G. Cohen, D. B. Kaplan, and A. E. Nelson, "Effective field theory, black holes, and the cosmological constant," *Physical Review Letters*, vol. 82, no. 25, pp. 4971–4974, 1999.
- [41] H. Wei, "Pilgrim dark energy," *Classical and Quantum Gravity*, vol. 29, no. 17, Article ID 175008, 2012.
- [42] M. Sharif and A. Jawad, "Phantom-like generalized cosmic chaplygin gas and traversable wormhole solutions," *The European Physical Journal Plus*, vol. 129, no. 1, article 15, 2014.
- [43] F. S. N. Lobo, "Phantom energy traversable wormholes," *Physical Review D*, vol. 71, no. 8, Article ID 084011, 2005.
- [44] F. S. N. Lobo, "Phantom energy traversable wormholes," *Physical Review D*, vol. 71, no. 8, Article ID 084011, 2005.
- [45] S. Sushkov, "Wormholes supported by a phantom energy," *Physical Review D*, vol. 71, no. 4, Article ID 043520, 5 pages, 2005.
- [46] M. Sharif and A. Jawad, "Thermodynamics in closed universe with entropy corrections," *International Journal of Modern Physics D: Gravitation, Astrophysics, Cosmology*, vol. 22, no. 3, Article ID 1350014, 21 pages, 2013.
- [47] P. Martin-Moruno, "On the formalism of dark energy accretion onto black- and worm-holes," *Physics Letters B*, vol. 659, no. 1-2, pp. 40–44, 2008.
- [48] M. Jamil, M. A. Rashid, and A. Qadir, "Charged black holes in phantom cosmology," *The European Physical Journal C*, vol. 58, no. 2, pp. 325–329, 2008.

- [49] E. Babichev, S. Chernov, V. Dokuchaev, and Y. Eroshenko, "Ultrahard fluid and scalar field in the Kerr-Newman metric," *Physical Review D*, vol. 78, Article ID 104027, 2008.
- [50] J. Bhadra and U. Debnath, "Accretion of new variable modified Chaplygin gas and generalized cosmic Chaplygin gas onto Schwarzschild and Kerr-Newman black holes," *The European Physical Journal C*, vol. 72, article 1912, 2012.
- [51] V. Sahni and A. Starobinsky, "Reconstructing dark energy," *International Journal of Modern Physics D*, vol. 15, pp. 2105–2132, 2006.
- [52] H. M. Sadjadi, "On the second law of thermodynamics in modified Gauss-Bonnet gravity," *Physica Scripta*, vol. 83, no. 5, Article ID 055006, 2011.
- [53] M. Sharif and S. Rani, "Pilgrim dark energy in $f(T)$ gravity," *Journal of Experimental and Theoretical Physics*, vol. 119, no. 1, pp. 75–82, 2014.
- [54] S. Chattopadhyay, A. Jawad, D. Momeni, and R. Myrzakulov, "Pilgrim dark energy in $f(T, T_G)$ cosmology," *Astrophysics and Space Science*, vol. 353, no. 1, pp. 279–292, 2014.
- [55] R. R. Caldwell and E. V. Linder, "Limits of quintessence," *Physical Review Letters*, vol. 95, Article ID 141301, 2005.
- [56] V. Sahni, T. D. Saini, A. A. Starobinsky, and U. Alam, "Statefinder—a new geometrical diagnostic of dark energy," *JETP Letters*, vol. 77, no. 5, pp. 201–206, 2003.



Hindawi

Submit your manuscripts at
<http://www.hindawi.com>

